

Dynamic correlation length scales under isochronal conditions

R. Casalini, D. Fragiadakis, and C. M. Roland

Naval Research Laboratory, Chemistry Division, Code 6120, Washington DC 20375-5342, USA

(Received 8 December 2014; accepted 21 January 2015; published online 9 February 2015)

The origin of the dramatic changes in the behavior of liquids as they approach their vitreous state—increases of many orders of magnitude in dynamic time scales and transport properties—is a major unsolved problem in condensed matter. These changes are accompanied by greater dynamic heterogeneity, which refers to both spatial variation and spatial correlation of molecular mobilities. The question is whether the changing dynamics are coupled to this heterogeneity; that is, does the latter cause the former? To address this, we carried out the first nonlinear dielectric experiments at elevated hydrostatic pressures on two liquids, to measure the third-order harmonic component of their susceptibilities. We extract from this the number of dynamically correlated molecules for various state points and find that the dynamic correlation volume for non-associated liquids depends primarily on the relaxation time, sensibly independent of temperature and pressure. We support this result by molecular dynamic simulations showing that the maximum in the four-point dynamic susceptibility of density fluctuations is essentially invariant along isochrones for molecules that do not form hydrogen bonds. Our findings are consistent with dynamic cooperativity serving as the principal control parameter for the slowing down of molecular motions in supercooled materials. [<http://dx.doi.org/10.1063/1.4907371>]

I. INTRODUCTION

The dynamics of liquids approaching their vitreous state exhibits interesting effects, the most prominent being spectacular changes in viscosity and relaxation times: these quantities may increase several orders of magnitude for a few degrees cooling. Eventually, the response becomes so sluggish that the supercooled liquid behaves as a solid over laboratory time scales, and the material is now referred to as a glass. This super-Arrhenius slowing of molecular motions (i.e., the logarithm of the relaxation times increasing faster than linearly with reciprocal temperature) is concurrent with the growth of space-time correlations,^{1–3} as motion of a molecule increasingly requires adjustments of others. Inherent to spatial correlation of the molecular mobilities is dynamic heterogeneity, the spatial variation of the dynamics (different parts of the liquid relax differently) reflected in non-exponentiality of the relevant time-correlation function. The growth of transient order manifested as dynamic correlations is commensurate with the size of these dynamic heterogeneities, the latter having been measured experimentally.^{4,5} Relatedly, computer simulations of model liquids have found that for a given material, a correlation exists between the dynamic correlation volume and the breadth of the relaxation dispersion.⁶

Non-associated liquids, that is, liquids that lack hydrogen bonding and complex formation, exhibit a property referred to as isochronal superpositioning, whereby the shape (breadth) of the relaxation function depends only on the relaxation time, τ .^{7,8} Since the relaxation function reflects the distribution of molecular relaxation times (whose average is the τ measured experimentally), isochronal superpositioning implies that dynamic heterogeneity is intimately connected to τ . Of interest

herein is whether dynamic correlations and their growth might be the cause of, rather than only accompanying, the slowing down of the dynamics in the supercooled regime. The spatial extent of dynamic correlations exhibits power-law dependences on the relaxation time at constant (low) pressure, with the cooperativity extending to several intermolecular distances at the transition to the glassy state.¹ Such results suggest that dynamic correlations may serve as the control parameter governing vitrification.^{9–12} However, to test this idea requires determination of the dynamic length scale in a liquid for different thermodynamic conditions having equivalent molecular mobility. Whether the dynamic correlation volume is invariant for state points with constant τ is a key to solving the glass transition problem.¹³

II. EXPERIMENTAL

Samples for nonlinear dielectric experiments were contained within Teflon gaskets, 10–25 μm thickness, between polished steel parallel plates that served as the electrodes. This capacitor assembly was placed in a Manganin cell (Harwood Engineering) inside a Tenney environmental chamber. Pressure was applied via an Enerpac pump in combination with a Harwood pressure intensifier; an alkane mixture was used as the hydraulic fluid. The peak voltage for the nonlinear experiments was 273 V, yielding electric fields on the order of 10^7 m/V. A Novocontrol HVB 2000 dielectric analyzer was used for the measurements.

The molecular volumes were obtained from the published equations of state for propylene carbonate (PC)¹⁴ and propylene glycol (PG).¹⁵

Molecular dynamics (MD) simulations were carried out using GROMACS.¹⁶ We modeled two rigid, polar united-atom structures, with potential energies combining Lennard-Jones (6-12) and Coulomb interactions. One structure consisted of a hydrogen-bonded molecule with three sites representing methyl, oxygen, and hydroxyl hydrogen. The other was a two-site structure with the same dipole moment but no H atom (and thus non-associated). For details of the system, see Ref. 17. Larger system sizes were used herein ($N = 10\,000$ for the H-bonded and $N = 16\,000$ for the non-associated liquid).

III. RESULTS AND DISCUSSION

A. Quantifying dynamic correlation

A number of indirect methods have been proposed to estimate dynamic correlation volumes,^{18–22} but, at least in principle, precise determinations can be obtained from high-order correlation functions,^{1,23–26} such as the four-point dynamic susceptibility of the density fluctuations,

$$\chi_4(t) = \int \langle \rho(r_1, 0) \rho(r_1 + r_2, 0) \rho(r_1, t) \rho(r_1 + r_2, t) \rangle_{r_1} dr_2. \quad (1)$$

$\chi_4(t)$ exhibits a maximum at a time $t \sim \tau$, with the height of the maximum proportional to the number of molecules dynamically correlated over this time scale: $N_c = \max\{\chi_4\}$. At longer times, χ_4 decays to zero since there is no long-range, persistent order in an amorphous liquid. χ_4 can be calculated in computer simulations, although results for model glass formers are mixed. Karmakar *et al.*²⁷ found that τ and the dynamic length scale have different dependences on the system size used in the simulation, inconsistent with the two quantities being coupled. On the other hand, χ_4 calculated in the NVT ensemble for a Lennard-Jones model liquid²⁸ and the static length scale determined from point-to-set correlation functions (which measure the spatial extent of boundary effects)²⁹ were found to be correlated with the relaxation times.

Experimental determination of χ_4 for real materials is problematic, requiring the use of approximations. Berthier *et al.*¹⁰ expressed Eq. (1) in terms of its various contributions, deriving two equations,

$$\chi_4(t) = \frac{kT^2}{c_p} \left[\frac{\partial C(t)}{\partial T} \Big|_P \right]^2 + \chi_4^{NPH}(t) \quad (2)$$

and

$$\chi_4(t) = \frac{kT^2}{c_V} \left[\frac{\partial C(t)}{\partial T} \Big|_P \right]^2 + \rho^3 kT \kappa_T \left[\frac{\partial C(t)}{\partial \rho} \Big|_T \right]^2 + \chi_4^{NVE}(t). \quad (3)$$

In these equations, k is the Boltzmann constant, c_p and c_V are the respective isobaric and isochoric heat capacities, and κ_T is the isothermal compressibility. The last term in either Eq. (2) or Eq. (3) is not available from measurements, but the insight of Berthier *et al.*¹⁰ was the notion that both may be sufficiently small near T_g that they can be neglected, with the dynamic susceptibility then approximated as

$$\chi_4(t) \approx \frac{kT^2}{c_p} \left[\frac{\partial C(t)}{\partial T} \Big|_P \right]^2 \quad (4)$$

and

$$\chi_4(t) \approx \frac{kT^2}{c_V} \left[\frac{\partial C(t)}{\partial T} \Big|_P \right]^2 + \rho^3 kT \kappa_T \left[\frac{\partial C(t)}{\partial \rho} \Big|_T \right]^2. \quad (5)$$

These expressions, both underestimates of $\chi_4(t)$, should be nearly equal.

Equations (4) and (5) have been applied to many materials³⁰ but of interest herein are measurements extending to high pressures, which enable assessment of the relationship between N_c and τ . Analyses using Eq. (4) of four liquids, salol, polychlorinated biphenyl, PC, and a mixture of *o*-terphenyl and *o*-phenyl phenol,³¹ found that state points having different temperatures and pressures but the same relaxation time had the same correlation volume; that is, N_c is uniquely defined (to within $\sim 10\%$) by τ , or vice versa. Subsequently, from a similar analysis on dibutylphthalate,³² it was reported that at conditions of constant τ , N_c increased with pressure. A third study³³ used both Eqs. (4) and (5) and determined that N_c for *o*-terphenyl, glibenclamide, and phenylphthalindimethylether decreased with increasing P at fixed τ . Thus, three studies on 8 different liquids concluded that under isochronal conditions, the dynamic correlation volume was constant,³¹ increased,³² or decreased³³ with increasing pressure and temperature.

These discordant results are not because the behavior of N_c is material specific, but rather there are both fundamental and technical issues with the calculation of Eqs. (4) and (5). In simulations, χ_4 has a dependence both on the dynamics (Newtonian vs. Brownian) and the statistical ensemble (NVT, NPT, etc.).^{34,35} Moreover, it is unclear whether the heat capacity, the excess heat capacity (which isolates the configurational part relevant to structural relaxation), or the change in c_p or c_V at T_g should be used in applying Eqs. (2)–(5); furthermore, values for the glassy or non-configurational part of the heat capacity are rarely available at high pressures. The approximation equations also involve derivatives of interpolated data, which can introduce uncertainties into the calculation of N_c . Note that Eqs. (2) and (3) are equivalent, and their respective approximations differ only in the neglected last term, presumed to be negligible. However, in Ref. 33, N_c from Eqs. (4) and (5) differed by as much as 40%; that is, the difference between two small contributions was an appreciable amount of the total χ_4 . This indicates either a lack of precision in the calculation of the approximations to χ_4 or the assumption that χ_4^{NPH} and χ_4^{NVE} are small near T_g ³⁶ is incorrect (as has been found in simulations³⁷). Notwithstanding the source of the problems in applying Eqs. (4) and (5), the obtained results for the behavior of N_c under isochronal conditions are ambiguous, motivating the use of a different method.

Although the linear susceptibility does not detect the transient order associated with dynamic correlation, it has been argued that higher order correlation functions should be manifested in higher order (non-linear) susceptibilities.³⁸ An example is the non-linear magnetic response of spin glasses, which can detect transitions evident otherwise only in four-point correlation functions.³⁹ From scaling arguments applied to mode coupling theory, the response of liquids to external perturbations has been shown to be increasingly nonlinear

as the glass transition is approached.⁴⁰ The inference is that the non-linear susceptibility can be used to measure dynamic heterogeneity; specifically, the amplitude of the nonlinear dielectric susceptibility is proportional to N_c ,³⁸

$$N_c \propto |\chi_3| \frac{kT}{\epsilon_0 a^3 (\Delta\chi_1)^2}, \quad (6)$$

where ϵ_0 the permittivity of free space, a the molecular volume, $\Delta\chi_1$ the linear dielectric strength, and $|\chi_3|$ the modulus of the third-order susceptibility corresponding to polarization cubic in the applied field. The derivation of Eq. (6) is more intuitive than rigorous, and features in the nonlinear susceptibility interpreted in terms of dynamic correlation lengths can be obtained in mean-field models that lack length scales of any kind.^{41,42} Nevertheless, this equation has been applied by several groups to determine the variation of N_c at ambient pressure with T ^{43–45} and during aging.⁴⁶ The main result, that N_c grows on cooling towards T_g in accord with the behavior of the relaxation time, supports the identification of the peak in $|\chi_3|$ with the dynamic correlation volume.

B. Nonlinear dielectric results

We carried out non-linear dielectric measurements under high pressure on two liquids, PC and PG. PC is a non-associated liquid conforming to isochronal superpositioning,^{7,8} whereas PG is hydrogen-bonded and thus its relaxation spectrum is not constant for constant τ .⁴⁷ In Figure 1 are representative $|\chi_3|$ spectra obtained at various pressures. For both liquids, there is an increase in the peak intensity with

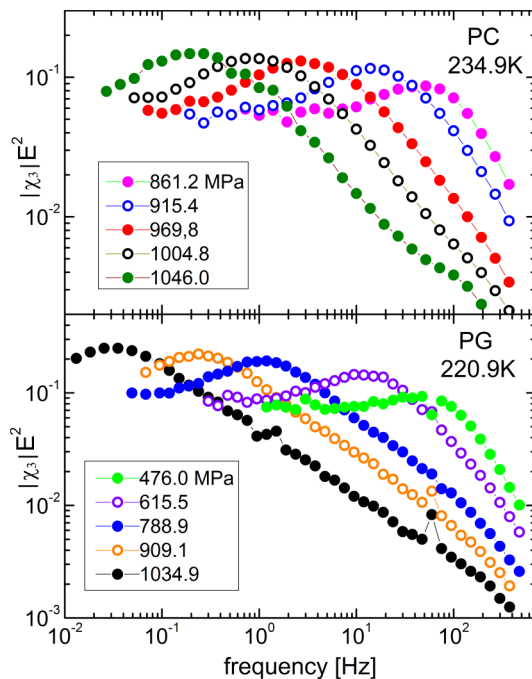


FIG. 1. Representative third-order harmonic spectra of PC (top) and PG (bottom) at the indicated temperature and pressures, the latter increasing from right to left. The electric field, E , was 8 MV/m (rms).

decrease in peak frequency, consistent with growth in the correlation volume as the relaxation time becomes longer.

To quantify the dynamic correlations requires that the contribution to $|\chi_3|$ from saturation of the dipole orientation be removed from the spectra. This saturation effect can be calculated assuming independent, rigid dipoles,^{43,48}

$$\chi_3^{sat}(\omega) = \frac{-3\epsilon_0 a^3 (\Delta\chi_1)^2}{5kT} \times \int_0^\infty g_{HN} \frac{3 - 17\omega^2\tau_0^2 + i\omega\tau_0(14 - 6\omega^2\tau_0^2)}{(1 + \omega^2\tau_0^2)(9 + 4\omega^2\tau_0^2)(1 + 9\omega^2\tau_0^2)} d\tau. \quad (7)$$

The distribution of relaxation times (heterogeneous dynamics) is described using the Havriliak-Negami function⁴⁹

$$g_{HN}(\ln \tau) = \frac{(\tau/\tau_0)^{\alpha\beta} \sin \beta\theta}{\pi((\tau/\tau_0)^{2\alpha} + 2(\tau/\tau_0)^\alpha \cos \pi\alpha + 1)^{\beta/2}}, \quad (8)$$

where

$$\theta = \arctan \left(\frac{\sin \pi\alpha}{(\tau/\tau_0)^\alpha + \cos \pi\alpha} \right). \quad (9)$$

In the above, α and β are constants. We fit the linear dielectric loss peaks to Eq. (8), then calculate the saturation effect using Eq. (7); typical results are shown in Figure 2. The difference spectrum can be used to extract N_c via Eq. (6).

As seen in Fig. 2, the saturation effect decays rapidly with frequency. This suggests a simpler method to avoid this interference, using a value of $|\chi_3|$ at higher frequencies than the peak. Brun *et al.*⁴⁴ have shown that $|\chi_3|$ at a frequency 2.5 times f_{max} , the frequency of the maximum in the linear dielectric loss, provides a measure of N_c unaffected by dipole saturation. In the inset to Fig. 2, we show the results for N_c of PC at ambient pressure obtained after correcting $|\chi_3|$ using Eq. (7) and by taking the value of $|\chi_3|$ at $2.5f_{max}$. Both values have similar temperature dependences, so that

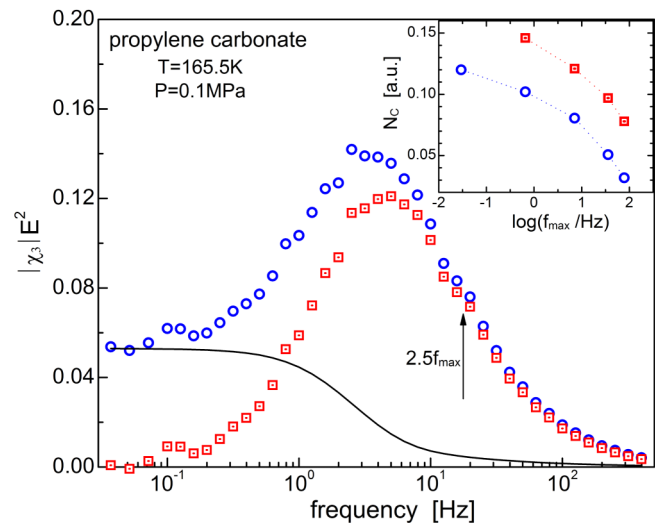


FIG. 2. Third-order spectrum of PC as measured (circles) and after subtraction of the saturation effect (squares), the latter indicated by the solid line. Inset shows the magnitude at $2.5f_{max}$ in the uncorrected spectrum (circles) and at the peak of the corrected spectrum (squares).

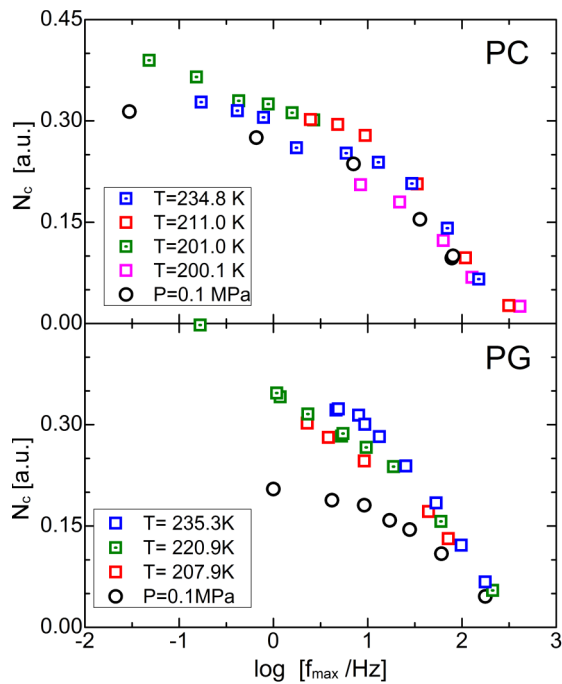


FIG. 3. Number of dynamically correlated molecules (arbitrary units) for PC (top) and PG (bottom) as a function of the frequency of the loss peak in the linear spectrum. The axes scales are the same for both panels.

either method yields a quantity proportional to the correlation volume. Hereafter, we report $|\chi_3(2.5f_{\max})|$.

In Figure 3 are N_c for the two liquids plotted as a function of the linear relaxation frequency. The data for PC show the two regimes expected for dynamic correlations—power-law dependences with a steeper slope at higher frequencies.¹⁰ This supports the interpretation of the peak in the nonlinear susceptibility in terms of dynamic correlations. Within the experimental scatter (ca. 15%), the number of dynamically correlated molecules for PC depends mainly on the relaxation time; there is no systematic variation in N_c with T or P . We can also arrive at this result without any analysis, by simply comparing $|\chi_3|$ for two state points having the same peak frequency in their linear spectra. As seen in Figure 4, these $|\chi_3|$ spectra for PC superpose; thus, the isochronal N_c are essentially constant.

PG is an associated liquid and therefore is expected to behave differently. The results in Fig. 3 bear this out: there are substantial variations (>50%) in N_c for a given τ . The data indicate a systematic increase in the correlation volume with increasing temperature or pressure at constant τ . The origin of this behavior is the change in H-bonding with thermodynamic conditions, whereby the liquid structure is not constant for isochronal conditions. Thus, neither the amplitude of $|\chi_3|$ nor the spectrum (Fig. 4) is invariant to changes in T and P , even when τ remains constant.

C. Molecular dynamics simulations

As discussed above, the four-point dynamic susceptibility enables determination of N_c . MD simulations of Lennard-Jones particles found that the N_c from χ_4 was constant for

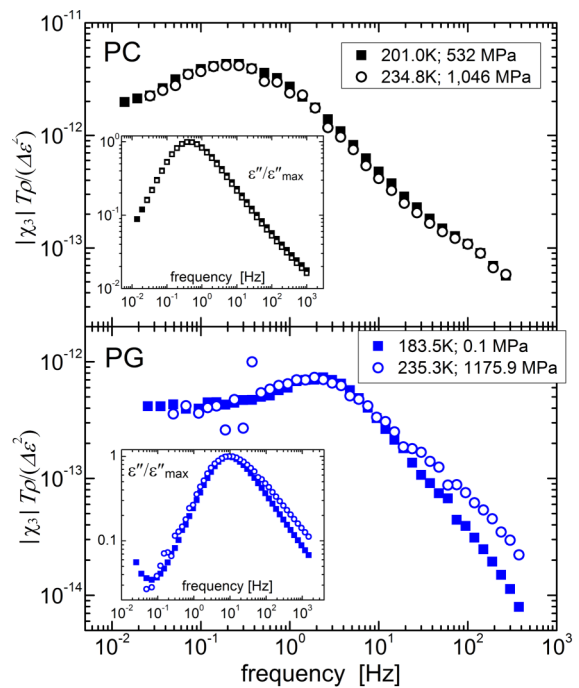


FIG. 4. $|\chi_3|$ spectra for PC (top) and PG (bottom) measured at conditions corresponding to constant linear relaxation time. Only for the non-associated liquid is isochronal superpositioning observed, both for the nonlinear and linear (inset) spectra.

constant τ .²⁸ This result is also predicted for simple liquids in the NVT ensemble,³⁵ “simple” defined as liquids displaying certain properties, such as isochronal superpositioning of the relaxation function. Accordingly, to compare with the dielectric results herein, we carried out MD simulations on two united-atom structures, modelling a three-site hydrogen-bonded molecule and a two-site structure with the same dipole moment but no H atom.

To compare the dielectric relaxation results, we calculated χ_4 for dipole reorientation in both the NVT and NPT ensembles. To calculate χ_4 in the NVT ensemble, we use the variance of the dipole autocorrelation function, $C_1(t)$ (rather than Eq. (1), the 4-point correlation function for density fluctuations),

$$\chi_4^{NVT}(t) = N \left[\langle C_1(t)^2 \rangle - \langle C_1(t) \rangle^2 \right]. \quad (10)$$

Adding a term for density fluctuations,¹⁰ we obtain χ_4 in the NPT ensemble,

$$\chi_4^{NPT}(t) = \chi_4^{NVT} + \rho^3 k T \kappa_T \left[\frac{\partial C_1(t)}{\partial \rho} \right]_T^2. \quad (11)$$

The linear susceptibility, which is unaffected by fluctuations and thus is the same for the two ensembles, was calculated as

$$\chi(\omega) = \chi'(\omega) + i\chi''(\omega) = 1 + i\omega \int_0^\infty e^{i\omega t} C_1(t) dt. \quad (12)$$

This allows comparison of the loss spectra at various state points at constant relaxation time, as done for the experimental dielectric spectra.

χ_4 determined for the NVT and NPT ensembles for the non-associated liquid at four isochronal state points are shown in Figure 5. The peak heights, and thus N_c , are constant to

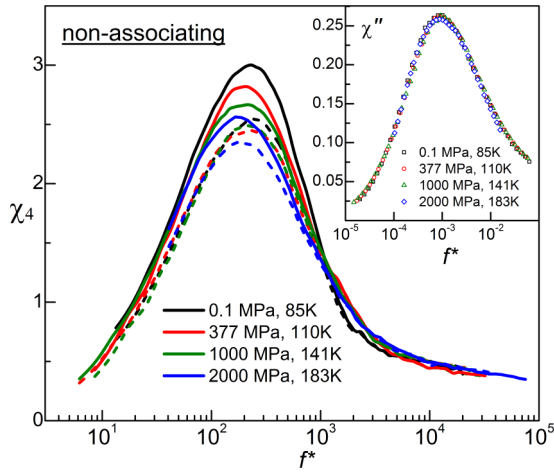


FIG. 5. χ_4 in the NVT (dashed lines) and NPT (solid lines) ensembles for the dipole autocorrelation function for a polar, non-associated liquid at three state points having equal reduced relaxation times ($\tau^* = \rho^{1/3}(kT)^{1/2}\tau$). T and P top to bottom; densities vary from 1.054 to 1.254. The inset shows the linear susceptibility for the same state points. The abscissa is the reduced frequency, $f^* = \rho^{-1/3}(kT)^{-1/2}f$.

within 4% for χ_4^{NVT} and 14% for χ_4^{NPT} , for density variations as large as 19%. For the H-bonded structure (Figure 6), this variation under isochronal conditions is much larger, χ_4 changing by as much as a factor of two. Similarly, there is a breakdown of isochronal superpositioning, as shown in the inset to Fig. 6. The very different behaviors of the non-associated and the H-bonded materials corroborate the nonlinear dielectric determination that for propylene carbonate, but not for the H-bonded propylene glycol, N_c is sensibly constant at constant τ . This behavior is consistent with isochronal superpositioning of the linear relaxation function for PC, but not for PG.

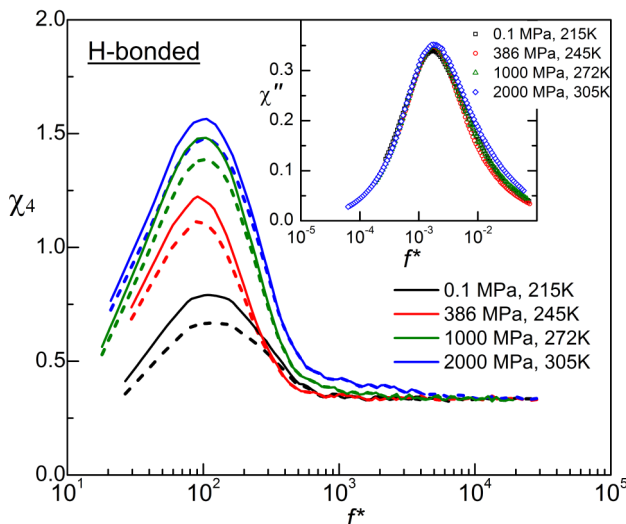


FIG. 6. χ_4 in the NVT (dashed lines) and NPT (solid lines) ensembles for the dipole autocorrelation function for a hydrogen-bonded liquid at four state points having equal reduced relaxation times. T and P decrease from top to bottom; densities for the same state points vary from 0.926 to 1.245. Inset shows departure of linear susceptibility from isochronal superpositioning.

D. Dynamic correlation and the temperature dependence of τ

If N_c and the distribution of relaxation times (the latter reflected in the breadth of the relaxation peak) are both functions of the relaxation time (i.e., constant for isochronal conditions), it follows that both comply with density scaling,^{50–54} whereby a dynamic property depends only on the ratio T/ρ^γ for any thermodynamic state point. Thus, for the relaxation time and N_c ,

$$\begin{aligned}\tau &= f(T\rho^{-\gamma}), \\ N_c &= g(T\rho^{-\gamma}),\end{aligned}\quad (13)$$

where f and g represent functions. Since the scaling exponent γ is a material constant that can be obtained from static, physical quantities,⁵⁵ the possibility exists to quantify the effect of changing thermodynamic conditions on dynamic heterogeneity from measurements limited to ambient pressure.

Recently, Bauer *et al.*⁵⁶ employed nonlinear dielectric measurements to obtain $|\chi_3|$ for four liquids at ambient pressure. From these data, they concluded that N_c and the apparent activation energy for the relaxation time at constant pressure exhibit direct proportionality, i.e.,

$$\left. \frac{d \ln \tau}{dT} \right|_P = AN_c \quad (14)$$

in which A is a constant, at least for isobaric conditions. If correct, this result would support the notion that dynamic heterogeneity directly causes the dramatic change in relaxation properties as liquids approach T_g . We test this idea herein, by comparing at different pressures the change of N_c for PC with temperature to E_a . The error in the latter is large since our measurements are for varying pressures at fixed temperature. For this reason, we derive an expression for the isobaric activation energy in terms of the activation volume, $\Delta V = \ln(10)RT \left. \frac{d \log \tau}{dP} \right|_T$. The ratio of the isobaric and isochoric activation energies can be expressed in terms of the scaling exponent⁵⁰

$$\frac{E_a|_P}{E_a|_\rho} = 1 + \gamma\alpha_P T, \quad (15)$$

where α_P is the thermal expansion coefficient and γ is the density scaling exponent.^{52–54} Combining Eq. (15) with an expression for γ in terms of the compressibility,⁵⁷

$$\gamma = \frac{\Delta V}{\kappa_T E_a|_\rho} \quad (16)$$

gives

$$E_a|_P = \Delta V \frac{1 + \gamma\alpha_P T}{\gamma\kappa_T}. \quad (17)$$

From this expression, the pressure-dependence of the apparent activation energy for PC is obtained, from the (implicit) pressure-dependences of ΔV , α_P , and κ_T . Results are shown for two temperatures in Figure 7. Included in the figure are the N_c data, which show some systematic deviations from strict proportionality with the activation energy. This implies that the proportionality constant A in Eq. (14) must be pressure-dependent.

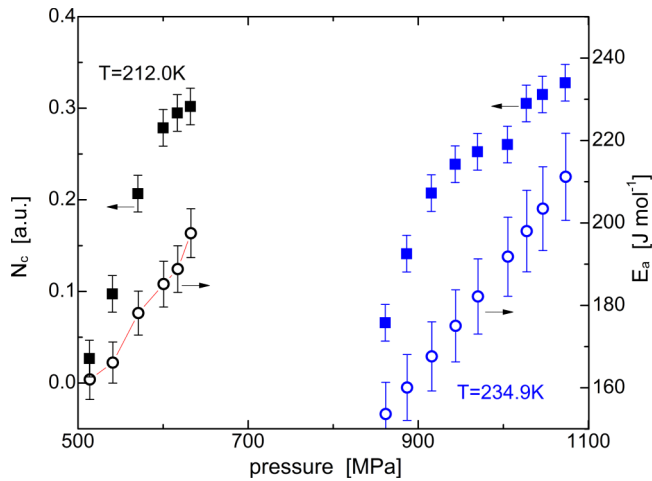


FIG. 7. Comparison of the temperature-dependence of the number of dynamically correlated molecules (filled squares) and the apparent activation energy (open circles) for PC at the indicated temperatures.

To corroborate the results in Fig. 7 more generally, we can make use of the scaling property. Taking the derivative of Eq. (13) yields

$$(T + \gamma\alpha_P T^2)^{-1} \frac{\partial \ln \tau}{\partial T^{-1}} = h(T\rho^{-\gamma}), \quad (18)$$

where h is a function. Thus, the apparent activation energy does not density scale, and since N_c does, they cannot be proportional for all thermodynamic conditions.

More recently, Buchenau *et al.*⁵⁸ pointed out that the activation energy, or the related fragility, for a glass-forming material is affected not only by intermolecular cooperativity but also by anharmonicity of the interatomic potential. If correct, this too belies the expectation that the temperature dependences of N_c and E_a should be in proportion for all state points (unless anharmonicity contributes to the magnitude of N_c , as speculated in Ref. 58). Our results for PC in Fig. 4 suggest any contribution of anharmonicity to the dynamic correlation is negligible. For associated liquids in which a marked change in the intermolecular potential, and thus the anharmonicity, occurs at high pressures, a more marked decoupling of N_c and E_a is observed.

IV. CONCLUSION

For non-associated liquids, the third-order dielectric susceptibility and four-point dynamic susceptibility from MD simulations both reveal only a small ($\sim 10\%$) variation in the number of dynamically correlated molecules for state points having significant differences in density but the same relaxation time. Together with prior work showing a correlation between spatial variation of molecular mobilities and τ , this means that these two reflections of dynamic heterogeneity are fundamentally connected to the time scale of the dynamics time. This is important for development of a theory of the glass transition, since viable models that predict τ implicitly make simultaneous predictions for N_c and the distribution of relaxation times.

ACKNOWLEDGMENTS

This work was supported by the Office of Naval Research. We thank R. Richert for informative discussions on nonlinear dielectric spectroscopy.

- ¹*Dynamical Heterogeneities in Glasses, Colloids and Granular Materials*, edited by L. Berthier, G. Biroli, J.-P. Bouchaud, L. Cipelletti, and W. van Saarloos (Oxford University Press, 2011).
- ²S. Karmakar, C. Dasgupta, and S. Sastry, *Annu. Rev. Condens. Matter Phys.* **5**, 255-284 (2014).
- ³A. Montanari and G. Semerjian, *J. Stat. Phys.* **124**, 103-189 (2006).
- ⁴M. D. Ediger, *Annu. Rev. Phys. Chem.* **51**, 99-128 (2000).
- ⁵H. Sillescu, *J. Non-Cryst. Solids* **243**, 81-108 (1999).
- ⁶C. M. Roland, D. Fragiadakis, D. Coslovich, S. Capaccioli, and K. L. Ngai, *J. Chem. Phys.* **133**, 124507 (2010).
- ⁷C. M. Roland, R. Casalini, and M. Paluch, *Chem. Phys. Lett.* **367**, 259-264 (2003).
- ⁸K. L. Ngai, R. Casalini, S. Capaccioli, M. Paluch, and C. M. Roland, *J. Phys. Chem. B* **109**, 17356-17360 (2005).
- ⁹J. P. Garrahan and D. Chandler, *Proc. Natl. Acad. Sci. U. S. A.* **100**, 9710-9714 (2003).
- ¹⁰Chap. 1 in Ref. 1.
- ¹¹V. Lubchenko and P. G. Wolynes, *Annu. Rev. Phys. Chem.* **58**, 235-266 (2007).
- ¹²A. Montanari and G. Semerjian, *J. Stat. Phys.* **125**, 23-54 (2006).
- ¹³L. Berthier and G. Biroli, *Rev. Mod. Phys.* **83**, 587-645 (2011).
- ¹⁴S. Pawlus, R. Casalini, C. M. Roland, M. Paluch, S. J. Rzoska, and J. Ziolo, *Phys. Rev. E* **70**, 061501 (2004).
- ¹⁵R. Casalini and C. M. Roland, *J. Chem. Phys.* **119**, 11951-11956 (2003).
- ¹⁶B. Hess, C. Kutzner, D. van der Spoel, and E. Lindahl, *J. Chem. Theory Comput.* **4**, 435-447 (2008).
- ¹⁷D. Fragiadakis and C. M. Roland, *J. Chem. Phys.* **138**, 12A502 (2013).
- ¹⁸F. Donth, *J. Non-Cryst. Solids* **53**, 325-330 (1982).
- ¹⁹A. Saiter, L. Delbreilh, H. Couderc, K. Arabeche, A. Schönhals, and J. M. Saiter, *Phys. Rev. E* **81**, 041805 (2010); A. Saiter, D. Prevosto, E. Passaglia, H. Couderc, L. Delbreilh, and J. M. Saiter, *ibid.* **88**, 042605 (2013).
- ²⁰F. Kremer, A. Huwe, M. Arndt, P. Behrens, and W. Schwieger, *J. Phys.: Condens. Matter* **11**, A175-A188 (1999).
- ²¹L. Hong, P. D. Gujrati, V. N. Novikov, and A. P. Sokolov, *J. Chem. Phys.* **131**, 194511 (2009).
- ²²A. Schönhals and E. Schlosser, *Phys. Scr. T* **49A**, 233-236 (1993).
- ²³C. Dasgupta, A. V. Indrani, S. Ramaswamy, and M. K. Phani, *Europhys. Lett.* **15**, 307-312 (1991).
- ²⁴L. Berthier, G. Biroli, J.-P. Bouchaud, L. Cipelletti, D. E. Masri, D. L'Hôte, F. Ladieu, and M. Pierno, *Science* **310**, 1797-1800 (2005).
- ²⁵S. Franz, C. Donati, G. Parisi, and S. C. Glotzer, *Philos. Mag. B* **79**, 1827-1831 (1999).
- ²⁶C. Bennemann, C. Donati, J. Baschnagel, and S. C. Glotzer, *Nature* **399**, 246-249 (1999).
- ²⁷S. Karmakar, C. Dasgupta, and S. Sastry, *Proc. Natl. Acad. Sci.* **106**, 3675-3679 (2009).
- ²⁸D. Coslovich and C. M. Roland, *J. Chem. Phys.* **131**, 151103 (2009).
- ²⁹G. M. Hocky, T. E. Markland, and D. R. Reichman, *Phys. Rev. Lett.* **108**, 225506 (2012).
- ³⁰S. Capaccioli, G. Ruocco, and F. Zamponi, *J. Phys. Chem. B* **112**, 10652-10658 (2008).
- ³¹D. Fragiadakis, R. Casalini, and C. M. Roland, *J. Phys. Chem. B* **113**, 13134-13137 (2009).
- ³²C. Alba-Simionesco, C. Dalle-Ferrier, and G. Tarjus, *AIP Conf. Proc.* **1518**, 527-535 (2013).
- ³³K. Koperwas, A. Grzybowski, K. Grzybowska, Z. Wojnarowska, A. P. Sokolov, and M. Paluch, *Phys. Rev. Lett.* **111**, 125701 (2013).
- ³⁴L. Berthier, G. Biroli, J.-P. Bouchaud, W. Kob, K. Miyazaki, and D. R. Reichman, *J. Chem. Phys.* **126**, 184503 (2007).
- ³⁵N. P. Bailey, T. B. Schröder, and J. C. Dyre, *Phys. Rev. E* **90**, 042310 (2014).
- ³⁶C. Dalle-Ferrier, C. Thibierge, C. Alba-Simionesco, L. Berthier, G. Biroli, J.-P. Bouchaud, F. Ladieu, D. L'Hôte, and G. Tarjus, *Phys. Rev. E* **76**, 041510 (2007).
- ³⁷E. Flenner and G. Szamel, *J. Chem. Phys.* **138**, 12A523 (2013).
- ³⁸J.-P. Bouchaud and G. Biroli, *Phys. Rev. B* **72**, 064204 (2005).
- ³⁹K. H. Fischer and J. A. Hertz, *Spin Glasses* (Cambridge University Press, 1991).

- ⁴⁰M. Tarzia, G. Biroli, A. Lefèvre, and J. P. Bouchaud, *J. Chem. Phys.* **132**, 054501 (2010).
- ⁴¹G. Diezemann, *J. Chem. Phys.* **138**, 12A505 (2013).
- ⁴²C. Brun, C. Crauste-Thibierge, F. Ladieu, and D. L'Hôte, *J. Chem. Phys.* **134**, 194507 (2011).
- ⁴³C. Crauste-Thibierge, C. Brun, F. Ladieu, D. L'Hôte, G. Biroli, and J. P. Bouchaud, *Phys. Rev. Lett.* **104**, 165703 (2010).
- ⁴⁴C. Brun, F. Ladieu, D. L'Hôte, M. Tarzia, G. Biroli, and J. P. Bouchaud, *Phys. Rev. E* **84**, 104204 (2011).
- ⁴⁵T. Bauer, P. Lunkenheimer, S. Kastner, and A. Loidl, *Phys. Rev. Lett.* **110**, 107603 (2013).
- ⁴⁶C. Brun, F. Ladieu, D. L'Hôte, G. Biroli, and J. P. Bouchaud, *Phys. Rev. Lett.* **109**, 175702 (2012).
- ⁴⁷C. M. Roland, R. Casalini, R. Bergmann, and J. Mattsson, *Phys. Rev. B* **77**, 012201 (2008).
- ⁴⁸R. Richert, *Phys. Rev. E* **88**, 062313 (2013).
- ⁴⁹R. Zorn, *J. Polym. Sci. Part B: Polym. Phys.* **37**, 1043-1044 (1999).
- ⁵⁰C. M. Roland, *Viscoelastic Behavior of Rubbery Materials* (Oxford University Press, 2011).
- ⁵¹C. M. Roland, S. Hensel-Bielowka, M. Paluch, and R. Casalini, *Rep. Prog. Phys.* **68**, 1405-1478 (2005).
- ⁵²R. Casalini and C. M. Roland, *Phys. Rev. E* **69**, 062501 (2004).
- ⁵³C. Dreyfus, A. L. Grand, J. Gapinski, W. Steffen, and A. Patkowski, *Eur. Phys. J. B* **42**, 309-319 (2004).
- ⁵⁴C. Alba-Simionesco, A. Cailliaux, A. Alegria, and G. Tarjus, *Europhys. Lett.* **68**, 58-64 (2004).
- ⁵⁵R. Casalini and C. M. Roland, *Phys. Rev. Lett.* **113**, 085701 (2014).
- ⁵⁶T. Bauer, P. Lunkenheimer, and A. Loidl, *Phys. Rev. Lett.* **111**, 225702 (2013).
- ⁵⁷R. Casalini and S. Bair, *J. Chem. Phys.* **128**, 084511 (2008).
- ⁵⁸U. Buchenau, R. Zorn, and M. A. Ramos, *Phys. Rev. E* **90**, 042312 (2014).